Supplement of Ocean Sci., 22, 3747–3770, 2026
https://doi.org/10.5194/os-22-3747-2026-supplement
© Author(s) 2026. CC BY 4.0 License.



Ocean Science Open Access EGU

Supplement of

Simulated Antarctic iceberg melting occurs primarily within the Southern Ocean mixed layer

Anna Olivé Abelló et al.

Correspondence to: Anna Olivé Abelló (anna.olive-abello@univ-grenoble-alpes.fr) and Nicolas C. Jourdain (nicolas.jourdain@univ-grenoble-alpes.fr)

The copyright of individual parts of the supplement might differ from the article licence.

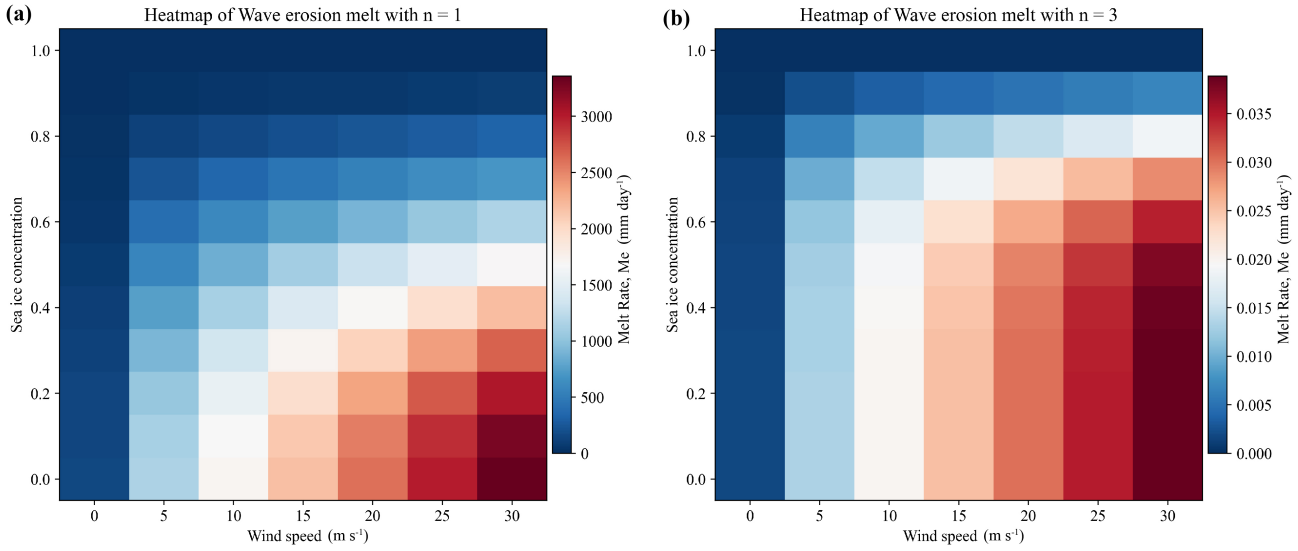


Figure S1. Wave-induced ablation as a function of wind speed and sea-ice concentration for (a) $n = 1$ and (b) $n = 3$ in Eq. (3) of the main article.

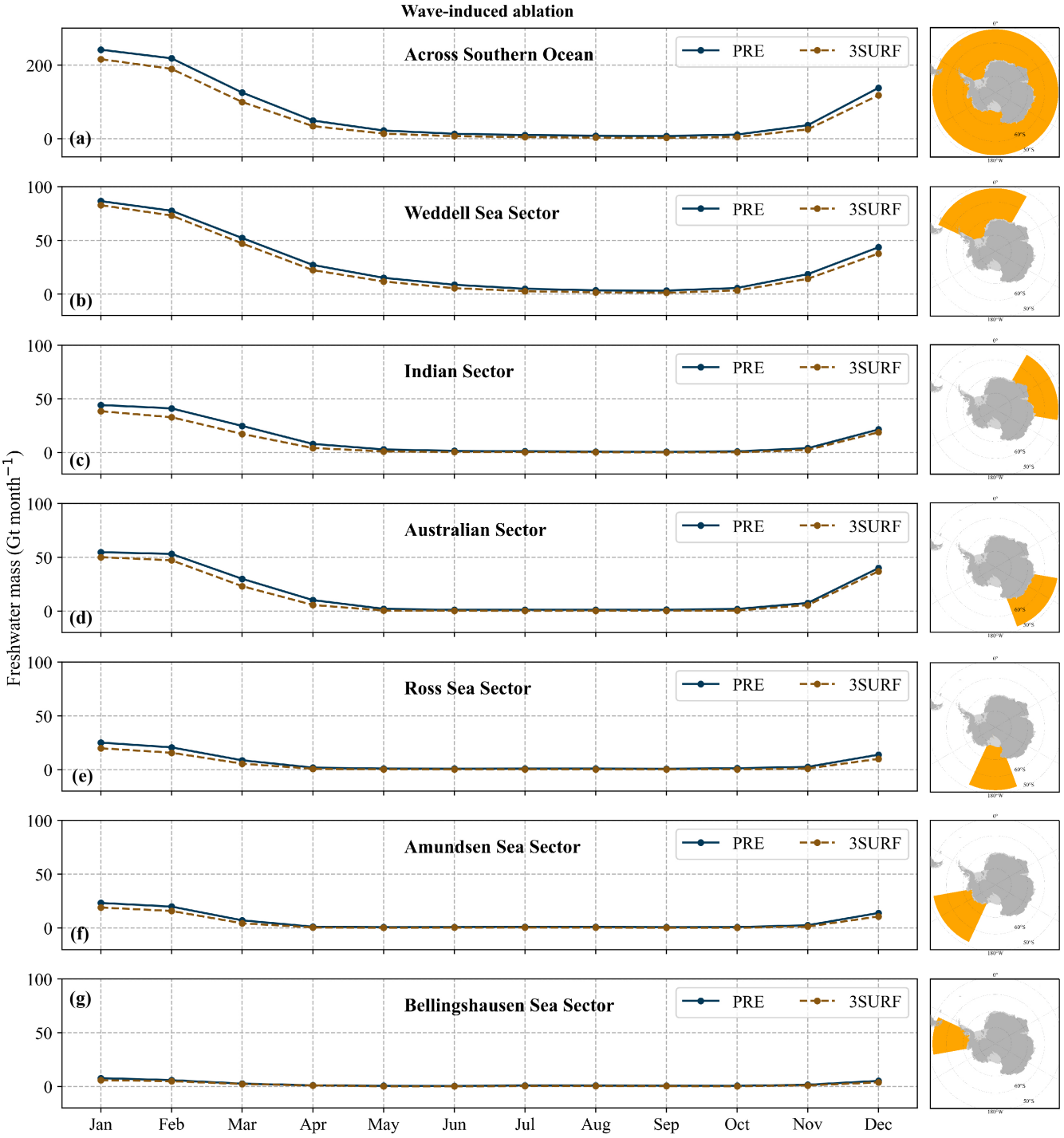


Figure S2. Monthly climatology of iceberg wave-induced ablation in the PRE (blue solid line) and 3SURF (brown dahed line) experiments (a) across the Southern Ocean, (b) the Weddell Sea, (c) Indian, (d) Australian, (e) Ross Sea, (f) Amundsen Sea, and (g) Bellingshausen Sea sectors (following the regions defined in Figure 1).

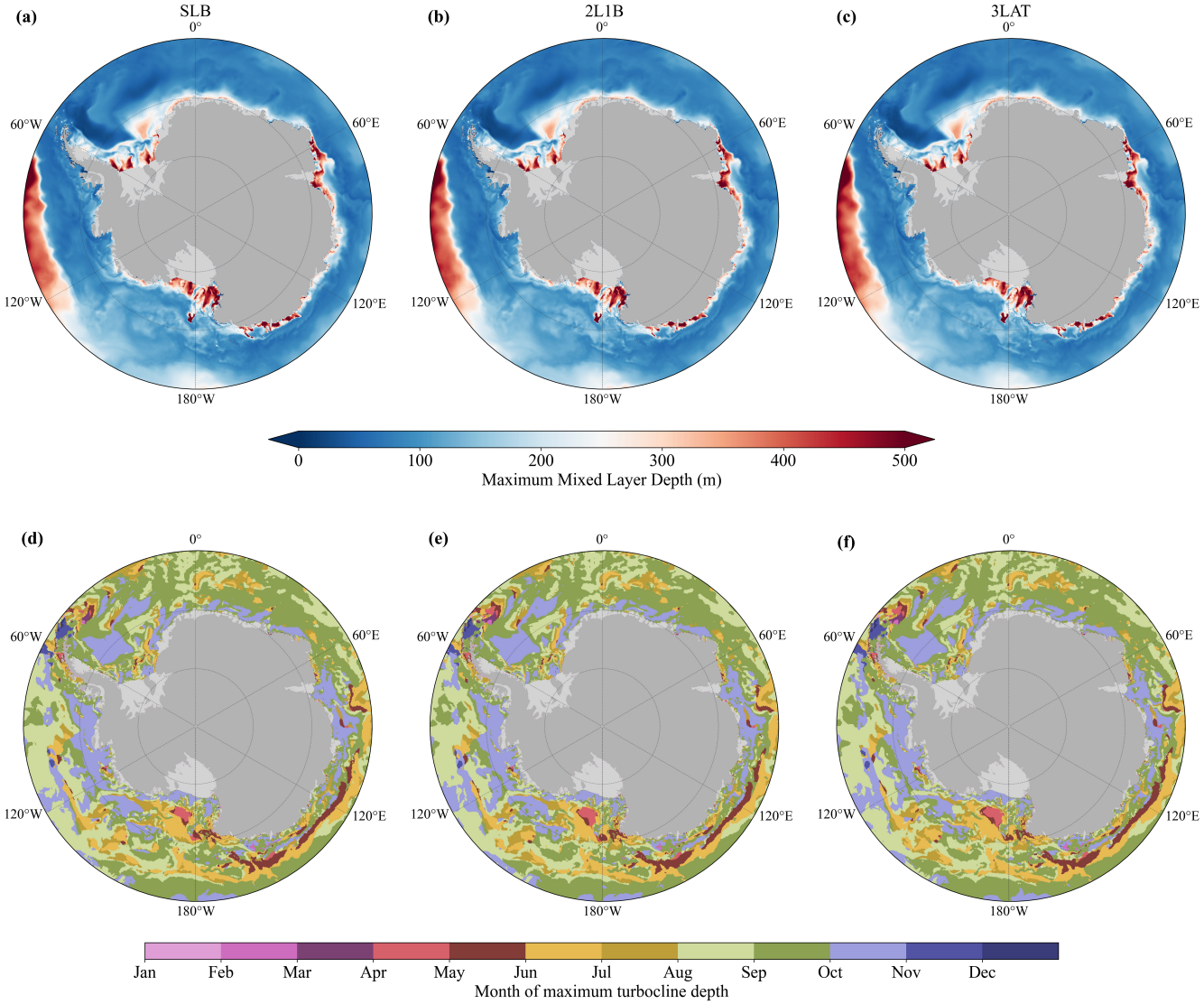


Figure S3. Spatial distribution of the 15-year mean annual maximum mixing layer depth (m) and the corresponding month of occurrence for (a,d) SLB, (b,e) 2L1B and (c,f) 3LAT.

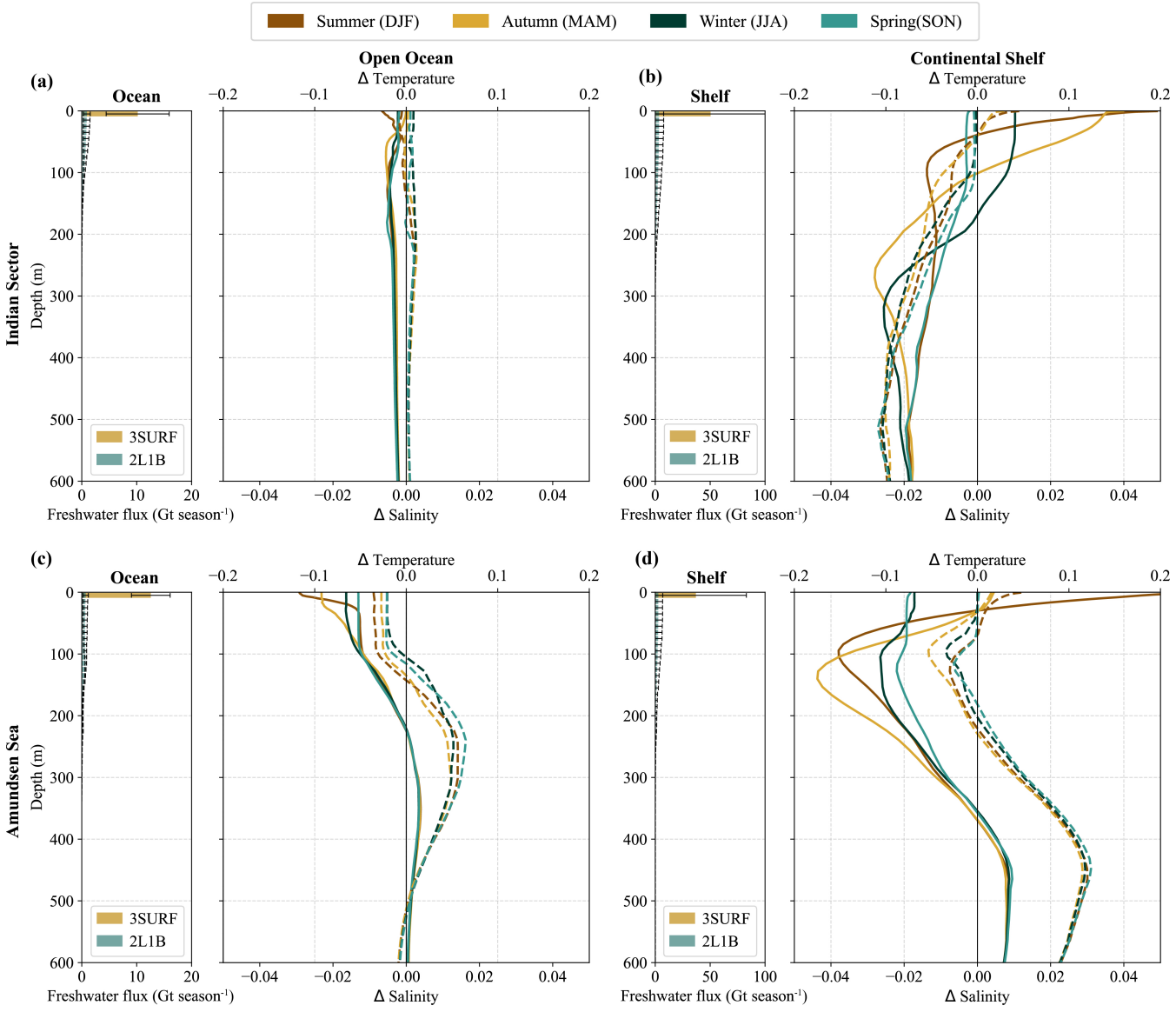


Figure S4. 15-year seasonal mean temperature and salinity profiles obtained from the difference between the 2L1B and 3SURF experiments (2L1B - 3SURF) over the Antarctic continental shelf and offshore in (a, b) the Indian and (c, d) Amundsen sectors. Temperature is shown with dashed lines and salinity with solid lines. Insets show the corresponding freshwater flux (Gt per season) released over each domain (continental shelf or open ocean) for the 2L1B and 3SURF experiments.

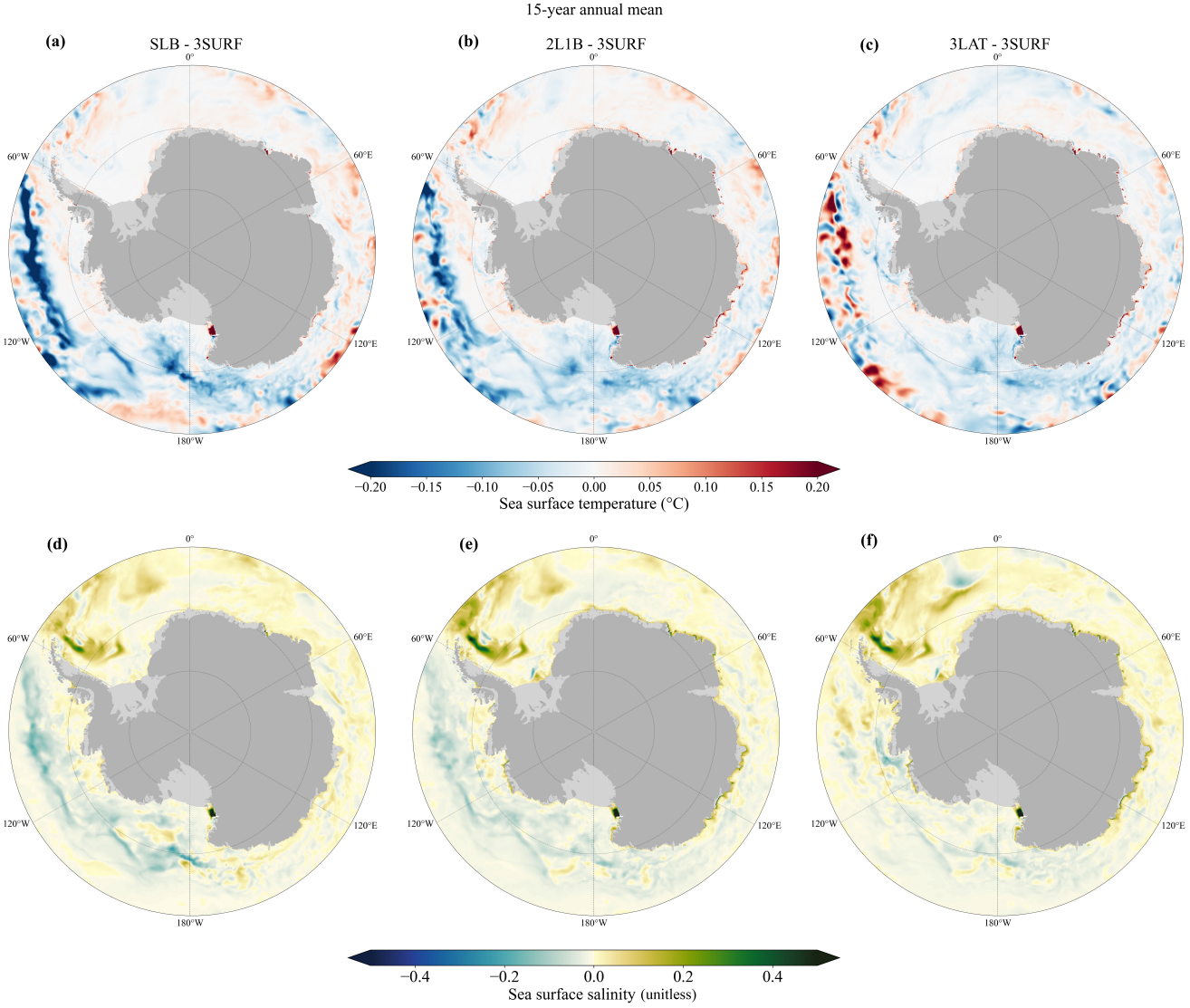


Figure S5. Distribution of 15-year mean differences in (a–c) sea surface temperature and (d–f) sea surface salinity for the SLB, 2L1B, and 3LAT experiments relative to 3SURF.

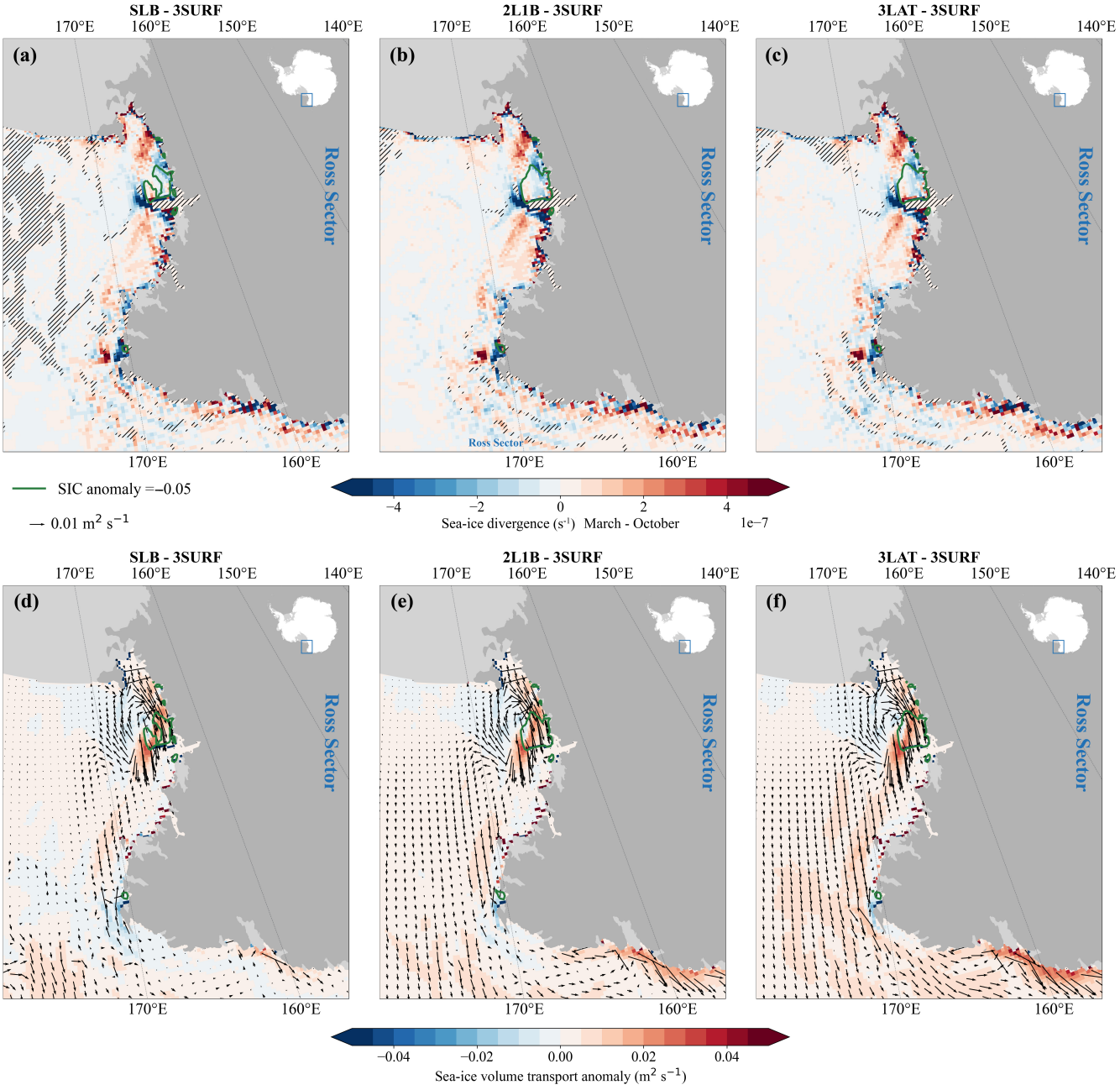


Figure S6. Sea-ice divergence (s^{-1}) and volume transport anomalies ($m^2\ s^{-1}$) averaged from March to October for (a,d) SLB, (b,e) 2L1B, and (c,f) 3LAT relative to 3SURF in the western Ross Sea. Sea-ice volume transport is calculated as the sea-ice volume per unit grid-cell area multiplied by the sea-ice velocity, while arrows indicate the corresponding vector transport anomalies. Green contours indicate a sea-ice concentration anomaly of -0.05. Hatched areas in (a–c) indicate regions where mean differences are not statistically significant at the 95% confidence level. The blue box in the Antarctic inset indicates the location of the study region.

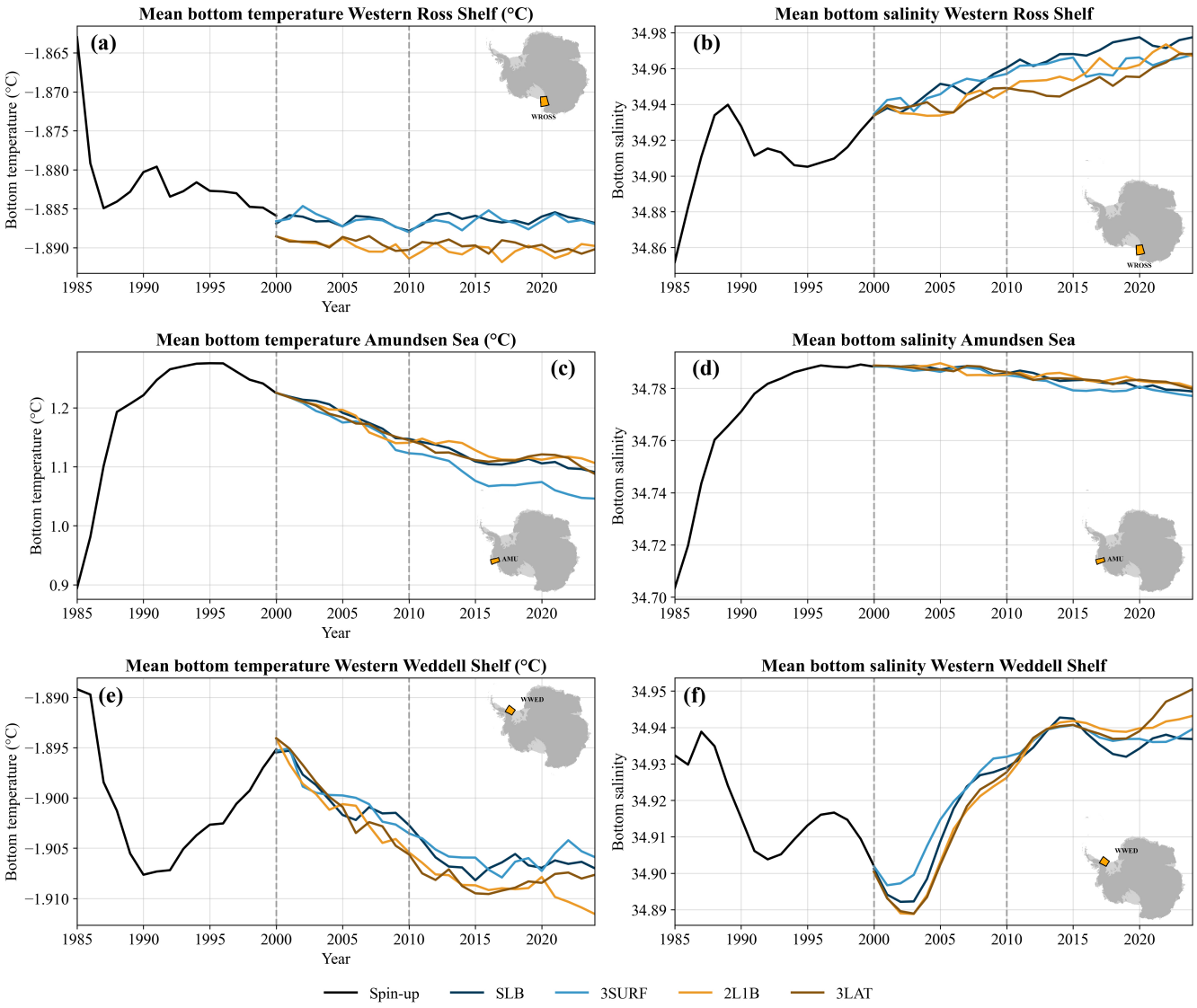


Figure S7. Mean bottom temperature and salinity evolution in the (a, b) western Ross Sea, (c, d) Amundsen Sea and (e, f) western Weddell Sea. The black line shows the 15-year spin-up simulation (1985–2000), while the coloured lines show the four sensitivity experiments (SLB, 3SURF, 2L1B, and 3LAT) over the subsequent 25-year simulations (2000–2024). The vertical dashed lines indicate the start of the sensitivity experiments and the beginning of the 15-year period used to compute the climatologies.

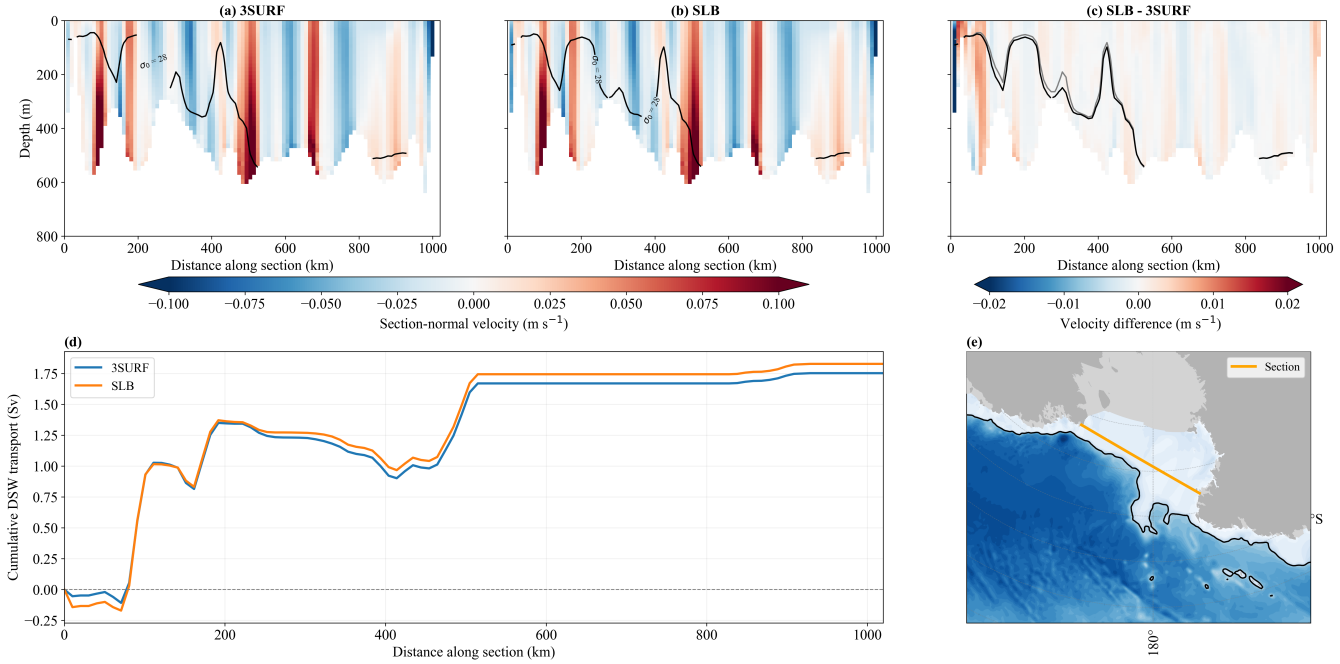


Figure S8. Section-normal velocity for (a) 3SURF and (b) SLB, and (c) their difference (SLB - 3SURF), along the 1020-km section parallel to the Ross Sea continental shelf break. Black contours indicate the σ_0 = 28 kg m^{-3} isopycnal used to identify DSW (grey contours in panel c show its position in 3SURF for comparison). (d) Cumulative DSW transport along the section for 3SURF and SLB. (e) Location of the section along the Ross Sea continental shelf break. Positive velocities and transport represent offshore DSW export.